

Energy barrier scalings in driven systems

Craig E. Maloney^{1,2} and Daniel J. Lacks³

¹*Department of Physics, University of California, Santa Barbara, California 93106, USA*

²*Lawrence Livermore National Lab CMS/MSTD, Livermore, California 94550, USA*

³*Department of Chemical Engineering, Case Western Reserve University, Cleveland, Ohio 44106, USA*

(Received 24 August 2005; revised manuscript received 9 February 2006; published 26 June 2006)

Energy landscape mappings are performed for two different molecular systems under mechanical loads. Barrier heights are observed to scale as $\Delta U \sim \delta^{3/2}$, where δ is a residual load. Catastrophe theory predicts that this scaling should arise for vanishing δ ; however, this region is irrelevant in physical processes at finite temperature because thermal fluctuations cause the system to cross over the barrier before reaching the small- δ regime. Surprisingly, we find that the $\Delta U \sim \delta^{3/2}$ scaling is valid far beyond the vanishing δ regime described by catastrophe theory. We discuss how this scaling will therefore be relevant at finite temperatures and gives corrections to Eyring's theory for transition rates.

DOI: [10.1103/PhysRevE.73.061106](https://doi.org/10.1103/PhysRevE.73.061106)

PACS number(s): 05.70.Ln, 83.60.-a, 83.10.-y, 83.50.-v

I. INTRODUCTION

In a broad range of condensed matter systems, one is interested in the question of how some material responds to an external mechanical load. External loads cause liquids to flow, in Newtonian or various types of non-Newtonian flows. Glassy materials, composed of polymers, metals, or ceramics, can deform under mechanical loads, and the nature of the response to loads often dictates the choice of material in various industrial applications. In biological systems, the response of proteins to external loads governs aspects of cell adhesion and muscle function.

The nature of all of these responses depends on both the temperature and loading rate. As described by Eyring [1], mechanical loading lowers energy barriers, thus facilitating progress over the barrier by random thermal fluctuations. The Eyring model approximates the loading dependence of the barrier height as linear. The Eyring model, with this linear barrier height dependence on load, has been used over a large fraction of the last century to describe the response of a wide range of systems [2] and underlies modern approaches to biophysical rupture processes [3–5], sheared glasses [6,7], etc.

The linear dependence will always correctly describe small changes in the barrier height, since it is simply the first term in the Taylor expansion of the barrier height as a function of load. It is thus appropriate when the barrier height changes only slightly before the system escapes the local energy minimum. This situation occurs at higher temperatures; for example, Newtonian flow is obtained in the Eyring model in the limit where the system experiences only small changes in the barrier height before thermally escaping the energy minimum.

As the temperature decreases, larger changes in the barrier height occur before the system escapes the energy minimum (giving rise to, for example, non-Newtonian flow). In this regime, the linear dependence is not necessarily appropriate, and can lead to inaccurate modeling. For example, Li and Makarov [8] have shown that there is a nonlinear barrier height dependence in stretched proteins, and that the assumption of a linear dependence in the analysis of experimental results leads to inaccurate conclusions.

The present investigation addresses this load dependence of the barrier height. The analysis is based on the energy landscape formalism [9], which considers dynamics to be the sum of vibrational-like motion within energy minima and transitions between energy minima. Barriers are associated with saddle points that connect adjacent energy minima. In Sec. II we review some basic results from the theory of simple catastrophes and extend them to explain our subsequent numerical observations. In Sec. III we present our numerical observations for a simple analytical model potential energy surface (PES) in one dimension and our fully atomistic glassy solid and protein models. In Sec. IV we discuss how the barrier scalings impact rate theoretic approaches, and finally make some concluding remarks.

II. CATASTROPHE THEORY

In molecular systems, the energy is a smooth function of the internal degrees of freedom plus a control parameter (e.g., stress or strain) which describes the loading conditions.¹ As the control parameter is varied, any minimum in the landscape will flatten out in some direction as the minimum collides with a first-order saddle point [10–12] (see Fig. 1). This type of externally induced topological change in a function is known as a fold catastrophe [13].

It has long been appreciated that these fold catastrophes induce universal scalings of particular features of the PES in the limit where the minimum and saddle point are infinitesimally close together [13]. In this limit, the function has the lowest-order Taylor expansion²

$$U = -Ax^3 - Bx\delta \quad (1)$$

because the first-order term (in the internal degrees of freedom) is zero at a minimum or saddle point, and the second-

¹The smoothness underlies the results we present below, and differences would arise in discontinuous models [4,28].

²The irrelevant directions (orthogonal to the reaction coordinate) on the potential energy landscape can be taken into account in a straightforward way, entering quadratically. They do not change the scalings, and we do not discuss them further.

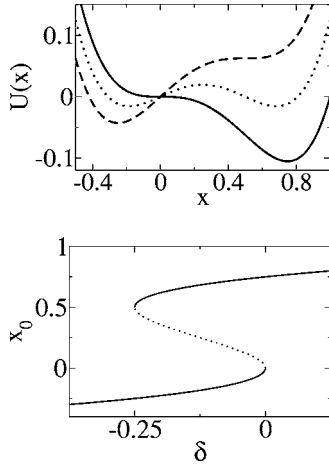


FIG. 1. Left: Energy from Eq. (8) for various δ . $\delta=0$, solid; $-1/8$, dotted; $-1/4$, dashed. Right: Bifurcation diagram indicating the locations of the extrema as a function of δ . Minima, solid; barrier, dotted. At $\delta=0$ the minimum of interest collides with a barrier. At $\delta=\delta_{\min}=-1/4$, the barrier collides with a distant minimum and ceases to exist; it makes no sense to discuss quantities such as ΔU for $\delta < \delta_{\min}$.

order term (projected along the direction that connects the minimum and barrier) is zero at the point where the minimum and saddle point collide. In Eq. (1), x is the projection of the system's coordinates onto the zero-curvature direction, δ is the control parameter's distance away from the singularity, and A and B are positive constants. To obtain the scaling laws, we note that the minimum and saddle point, x_- and x_+ , are the points where the energy derivative vanishes, the curvature along the reaction coordinate at the minimum and saddle point correspond to the second partial derivatives of the function, $\lambda_- = \frac{\partial^2 U}{\partial x^2}|_{x_-}$, $\lambda_+ = \frac{\partial^2 U}{\partial x^2}|_{x_+}$, and the height of the barrier, ΔU , corresponds to $\Delta U = U(x_+) - U(x_-)$. This analysis leads to the following scaling relations:

$$-x_- = x_+ = \sqrt{\frac{-B\delta}{3A}}, \quad (2)$$

$$\lambda_- = -\lambda_+ = 6A \sqrt{\frac{-B\delta}{3A}}, \quad (3)$$

$$\Delta U = 2A \left(\frac{-B\delta}{3A} \right)^{3/2}. \quad (4)$$

The fold ratio $r_f \doteq 6\Delta U / (2\lambda_- x_-^2)$ is unity when all three of these scaling relations are valid [14]. These arguments appeal only to δ 's role as a control parameter and are equally valid when δ represents, e.g., an imposed strain or stress. Recently, the consequences of these scalings have been discussed quantitatively in the context of phenomenological models [15–17]. Fold ratios in incipient catastrophes have been measured in molecular simulations [14], but the individual scaling relations have not previously been addressed in externally driven molecular level simulations.

These scaling relations must be obtained in the limit $\delta \rightarrow 0$, but at finite temperature, thermal fluctuations cause the barrier to be crossed before this vanishing- δ regime is being reached. Little attention has been paid to the accuracy of these scaling relations for the physically meaningful finite- δ regime. While the fold ratio has been shown to deviate significantly from unity at finite δ [14], the accuracy of the scaling relations for the individual quantities has not previously been addressed.

Clues to how the scaling breaks down at finite $|\delta|$ are obtained from a (1+1)-dimensional energy function $U(x, \delta)$, based on arguments similar to those given in [11]. The only requirement we make of U is that the coupling to the control parameter is bilinear over the region of interest: $U(x, \delta) = U_0(x) - B_0 x \delta$. Demanding that $(\partial U / \partial x)$ remain zero as we change δ requires that

$$\frac{d}{d\delta} \left(\frac{\partial U}{\partial x} \right) = \frac{\partial^2 U}{\partial x \partial \delta} + \left(\frac{dx_0}{d\delta} \right) \frac{\partial^2 U}{\partial x^2} \Bigg|_{x_0} \quad (5)$$

$$\Rightarrow \frac{dx_0}{d\delta} = \frac{B_0}{\lambda_0} \quad (6)$$

where x_0 is a stationary point. The energy of the stationary point then changes according to

$$\frac{dU}{d\delta} = \left(\frac{dx_0}{d\delta} \right) \frac{\partial U}{\partial x} \Bigg|_{x_0} + \frac{\partial U}{\partial \delta} = \frac{\partial U}{\partial \delta} = -B_0 x_0, \quad (7)$$

where the second equality follows from mechanical equilibrium. The fold scalings obey the above relations between the energy, position, and curvature of a stationary point, but these latter relations are more general because they are based on much weaker assumptions about the form of the energy function than the cubic form used to obtain the fold scalings. Since the energy barrier is obtained after two integrations of the inverse curvature, we anticipate that, as the load is backed away from the catastrophe, deviations from the scaling relations should occur first for the curvature, then for the position, and finally for the energy; i.e., the barrier height scaling should be more accurate at finite δ than the other scaling relations.

III. LANDSCAPE GEOMETRY

We first test this hypothesis regarding the relative accuracy of the barrier height scaling on a simple, analytically solvable model. This simple model includes the next-order term in the Taylor expansion for the energy, giving a fourth-order polynomial

$$U = -x^3 - x\delta + x^4. \quad (8)$$

The landscape for this energy function for various δ is shown in Fig. 1.³ As δ goes to zero, the (left hand) minimum and the energy barrier join together at $x=0$. As δ is backed away

³Prefactors on each of the three terms may be absorbed into a redefinition of length, energy, and δ .

from zero, the minimum and barrier move apart. As δ is backed further away from zero, the barrier eventually collides with some *other* minimum at $\delta=-1/4$, rendering the quantities ΔU , λ_+ , x_+ undefined. The results for this simple model are consistent with our expectation that the scaling of the barrier height will be more accurate than the scaling of the curvature: at the largest possible values of δ , the barrier height scaling remains accurate to within 10%, while the scaling for λ_- is in error by 100%, and the scaling prediction for λ_+ is infinite in error (λ_+ vanishes altogether). Analogous results are obtained with a negative fourth-order term, in which case the maximal $|\delta|$ occurs when the minimum collides with the other barrier (in this case λ_+ is at 50% of the value from the scaling relation, and λ_- vanishes altogether). Similar results are obtained for other simple, analytically solvable models.

We have tested these ideas in simulations of realistic atomistic models by tracking local minima and saddle points as a control parameter is varied. To check the generality of our arguments, we investigate two very different systems (a model glass and a model protein), and consider both strain and stress as control parameters.

The model glass simulations use the Stillinger-Weber 80:20 mixture [18], and include 500 particles in an orthorhombic simulation cell with periodic boundary conditions (the Stillinger-Weber functional form, which is similar to the Lennard-Jones potential, is used because continuous derivatives at a finite cutoff are necessary to analyze the energy landscape at the required precision). The glassy state was produced by a $T=0$ quench from an equilibrated liquid at a fixed density of 1.2. Strain was induced via volume-preserving uniaxial extension. For further details, see Ref. [19]. The model protein is the Thirumalai model [20], which consists of 46 sites that interact with bond stretching, angle bending, torsion, and nonbonded (Lennard-Jones) interactions. The starting configuration was the global energy minimum, located using techniques discussed elsewhere [12].

A minimum is tracked by repeatedly minimizing the energy as the control parameter is varied in small increments. Similarly, a saddle point is tracked by repeatedly minimizing the sum of the squares of the forces as the control parameter is varied in small increments (the saddle point is found initially by searching halfway along the vector that connects two minima). All numerical minimizations are performed using a variable metric algorithm, and the eigenvalues and eigenvectors of the system are computed using a standard QL reduction algorithm [21].

Results for the glass, with shear strain as the control parameter, are shown in Fig. 2. Since the system is multidimensional, it will have many eigenvalues at the minimum, and we take λ_- to be the smallest of these. The magnitude of the single negative eigenvalue at the barrier is denoted as λ_+ . We choose to use λ_- to compute the fold ratio.

In the small- δ limit all of the scaling relations [Eqs. (2), (3), and (4)] are accurate, and the fold ratio is unity. This behavior is of course expected, because the catastrophe is of the fold type. In terms of the large- δ behavior, the results are fully consistent with the ideas based on the arguments above. First, the barrier eigenvalue goes to zero at about $\gamma_c - \gamma \sim 0.007$ in a collision with some *other* minimum. Also, the

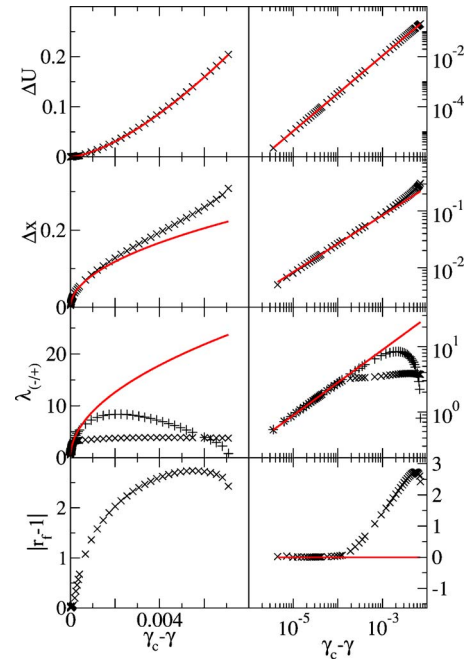


FIG. 2. (Color online) From top to bottom ΔU , Δx , λ_- (\times symbols) and λ_+ ($+$ symbols), and $|r_f - 1|$ upon approach to a typical catastrophe. The solid (red) lines are the theoretical scaling predictions [Eqs. (2)–(4)] with prefactors determined by a fit to the smallest two decades of $\gamma_c - \gamma$ shown. γ_c is determined via optimization of ΔU to the $(\gamma_c - \gamma)^{3/2}$ form.

accuracy of the scaling relation for the curvature (3) is quite poor in comparison with the accuracy of the scaling relation for the barrier height (4), with the barrier height scaling being a reasonable approximation over the entire interval up to $\gamma_c - \gamma \sim 0.007^4$.

For the protein model, the end to end distance of the protein, L , can be taken as the control parameter. As shown in Fig. 3, both increasing and decreasing L cause the lowest curvature at the minimum to go to zero, indicating the onset of catastrophes. As expected, the scaling relations are accurate at small values of δ , where δ is $L_c - L$ and L_c is the length at which the minimum and barrier collide. At large δ , the scaling relation for the curvature becomes poor while the scaling relation for the barrier height is reasonably accurate over the entire range of δ . In contrast to the Lennard-Jones case, it is the minimum that disappears in a collision with an extraneous barrier with λ_- going to zero at the maximal $L_c - L$, but, in both cases, the barrier scalings are found to be superior to the scalings of either of the curvatures.

To use force as a control parameter in the protein model, L is reinstated as a *bona fide* degree of freedom, and an external coupling is introduced so that $U_{\text{tot}} = U_{\text{int}} - FL$, where

⁴The sharp transition in λ_- in Fig. 2 can be understood in terms of multidimensional hybridization effects. Above $\gamma_c - \gamma \sim 10^{-4}$, other eigenmodes have eigenvalues that are lower than the curvature along the reaction coordinate, and it is only below $\gamma_c - \gamma \sim 10^{-4}$ that the reaction coordinate becomes a *bona fide* eigenmode. The eigenmode at the *barrier*, on the other hand, is always reasonably well aligned along the reaction coordinate.

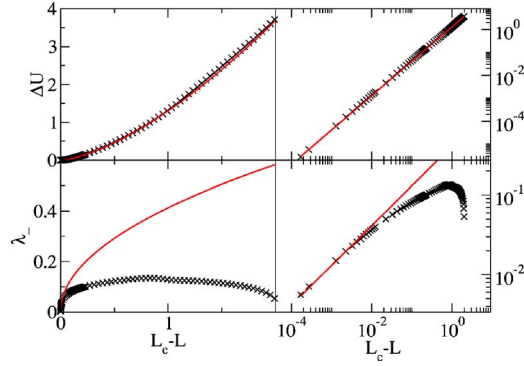


FIG. 3. (Color online) Top, ΔU , and bottom, λ_{\pm} , for the protein model in a length-controlled mode as functions of $L_c - L$ where L is the end to end length and L_c is the value of length at which the minimum and barrier collide.

U_{int} is the usual internal energy of the protein. As the arguments for the fold scaling relations appeal only to the smoothness of the energy function and not the particular mode of loading, we expect analogous results when force is the control parameter. ΔU and λ_{\pm} are plotted in Fig. 4. Again, all scaling relations are accurate at small δ , but at large δ the scaling relation for ΔU is much more accurate than the scaling relation for λ_{\pm} .

IV. RATE THEORY

In order to understand the behavior of a system under load, one often introduces a one-dimensional, overdamped Langevin equation, where the single spatial coordinate represents displacement of the system along its reaction coordinate. According to Kramers' theory [22], the rate at which the system makes a transition over the barrier is given by

$$k = \frac{\sqrt{-\lambda_+ \lambda_-}}{2\pi\gamma_b} \exp(-\Delta U/k_B T) \quad (9)$$

where k is the rate at which the system makes a transition, γ_b is the viscous bath coupling parameter, and λ_{\pm} and ΔU depend on the load. Eyring's theory [1] for transition rates in loaded molecular systems can be considered as a Kramers

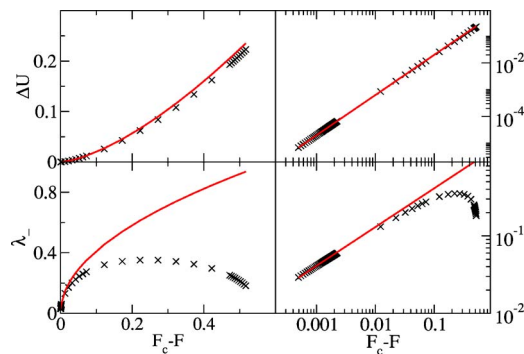


FIG. 4. (Color online) Top, ΔU , and bottom, λ_{\pm} , for the protein model, as functions of $F_c - F$ where F is the external force and F_c is the value of force at which the minimum and barrier collide.

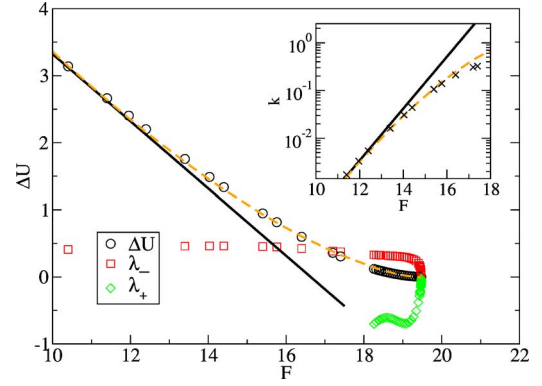


FIG. 5. (Color online) Landscape geometry and Kramers rates (inset) upon approach to the maximum force peak in the protein model. ΔU , circles (black); λ_{\pm} , squares (red); λ_+ , diamonds (green); fit to $\Delta U \sim \delta F$, solid (black); fit to $\Delta U \sim \delta F^{3/2}$, dashed (orange). Inset: True Kramers rate $(-\lambda_+ \lambda_-)^{1/2} \exp(-\Delta U/k_B T)$, \times 's (black); Eyring form, $\lambda_0 \exp[-a(F_c - F)/k_B T]$, solid (black); modified Eyring form, $\lambda_0 \exp[-a(F_c - F)^{3/2}/k_B T]$ dashed (orange). a and F_c are obtained from the fits shown in the main plot. λ_0 was taken to be 2.25.

theory with the further assumptions that the preexponential factor is not important and can be taken as constant and that the barrier height varies linearly with load. The Eyring theory, of course, must be a good approximation if the load only varies by a small amount before the system makes a transition.

Our results show that the linear load dependence approximation generically overestimates the transition rates since the proper scaling form $\Delta U \sim (F_c - F)^{3/2}$ goes to zero more slowly than linearly. To underscore the importance of this point, we consider the above rate theories in conjunction with results for the protein model. Figure 5 shows results for ΔU , λ_{\pm} , and both linear and $(F_c - F)^{3/2}$ fits for ΔU (note that these results are for a different barrier than shown in Fig. 4). The inset to Fig. 5 shows a comparison of transition rates calculated by the Kramers theory, Eq. (9), using (i) the actual measured values of λ and ΔU , (ii) the Eyring theory in which the preexponential factor is taken to be constant and ΔU decreases linearly with the load, and (iii) a modified Eyring theory in which the preexponential factor is taken to be constant and ΔU is given by a fit to the scaling form (4). The rates are given in units of the strength of the viscous bath coupling γ_b . To set an experimentally relevant energy scale, we evaluate the rates at the highest temperature for which the native protein structure is thermodynamically stable, $k_B T = 0.4$ (in dimensionless energy units) [23].

The first thing to note in Fig. 5 is that the barrier scaling Eq. (4) is again very accurate throughout the entire range of loading for which the barrier exists, while the curvature scalings do not become relevant until much nearer the catastrophe event; in fact the changes in the curvature are not even monotonic over the range on which the $(3/2)$ barrier scaling is accurate. From the inset to Fig. 5, it is clear that the modified Eyring form gives a much better approximation to the Kramers transition rates. The accuracy of the modified Eyring form is due to both the accuracy of the barrier scaling

over a large range of loads, and the fact that the curvatures only enter into Eq. (9) as a preexponential factor. Note that this analysis is carried out at the highest temperature for which the native protein state is stable, and thus the improvement of the modified Eyring form in comparison to the Eyring form will be even more significant at lower temperatures.

Several recent works [17,24–27] have focused on these deviations from Eyring behavior based on the scaling forms (2), (3), and (4). Johnson and Samwer [27] have argued along similar lines to us that the $(F_c - F)^{3/2}$ barrier scaling should lead to a $T^{2/3}$ dependence in the yield stress and gave experimental data from many different metallic glasses to support their claim. The authors needed to suppose that the (3/2) barrier scalings held over reasonably large intervals of load. The present work demonstrates precisely this.

Other studies focused on time-ramped loads. Dudko and co-workers [24], working in the context of an explicitly time-dependent load, showed how the scaling forms were necessary to collapse average rupture force data at differing temperatures and loads. Dias *et al.* [26] pointed out that the catastrophes in systems with high degrees of symmetry (in their case, a circular chain of bonds) need not be of fold type and could lead to scalings other than the (3/2) scaling of the fold catastrophe. Our results support the notion that the fold scalings are those that are relevant to more realistic molecular models.

V. SUMMARY

In summary, barrier heights in molecular systems are found to follow, to fairly high accuracy, the scaling relation $\Delta U \sim \delta^{3/2}$. While this scaling relation has been known to be rigorously valid in the $\delta \rightarrow 0$ limit, this vanishing- δ regime is not physically significant at finite temperature, because thermal fluctuations cause the system to cross the barrier before the low- δ regime is reached. However, our investigation shows that the scaling relation is appropriate outside of the low- δ limit—even when the scalings fail dramatically for the curvatures or the fold ratio. The barrier height scaling is relevant for all driven thermal systems, including flowing liquids, mechanically deformed glasses, and stretched proteins. Quantitative analyses of these driven thermal systems, based on modifications of Eyring’s theory to take the proper scalings of the barrier height into account, will lead to an improved understanding and description of these systems.

ACKNOWLEDGMENTS

We thank W. Johnson, M. Demkowicz, and A. Lemaître for useful discussions. C.E.M. was supported under the auspices of the U.S. Department of Energy by the University of California, Lawrence Livermore National Laboratory under Contract No. W-7405-Eng-48. D.J.L. was supported by the National Science Foundation under Grant No. DMR-0402867.

-
- [1] H. Eyring, *J. Chem. Phys.* **4**, 283 (1936).
 - [2] R. Larson, *The Structure and Rheology of Complex Fluids* (Oxford University Press, Oxford, 1998).
 - [3] G. I. Bell, *Science* **200**, 618 (1978).
 - [4] E. Evans and K. Ritchie, *Biophys. J.* **72**, 1541 (1997).
 - [5] D. Craig, M. Gao, K. Schulten, and V. Vogel, *Structure (London)* **12**, 21 (2004).
 - [6] A. S. Argon, *Acta Metall.* **27**, 47 (1979).
 - [7] J. Rottler and M. O. Robbins, *Phys. Rev. E* **68**, 011507 (2003).
 - [8] P. C. Li and D. E. Makarov, *J. Chem. Phys.* **119**, 9260 (2003).
 - [9] F. H. Stillinger and T. A. Weber, *Phys. Rev. A* **25**, 978 (1982).
 - [10] D. L. Malandro and D. J. Lacks, *Phys. Rev. Lett.* **81**, 5576 (1998).
 - [11] C. Maloney and A. Lemaître, *Phys. Rev. Lett.* **93**, 195501 (2004).
 - [12] D. J. Lacks, *Biophys. J.* **88**, 3494 (2005).
 - [13] V. Arnold, *Catastrophe Theory*, 3rd ed. (Spring-Verlag, Berlin, 1992).
 - [14] D. J. Wales, *Science* **293**, 2067 (2001).
 - [15] O. K. Dudko, A. E. Filippov, J. Klafter, and M. Urbakh, *Proc. Natl. Acad. Sci. U.S.A.* **100**, 11378 (2003).
 - [16] T. V. Bogdan and D. J. Wales, *J. Chem. Phys.* **120**, 11090 (2004).
 - [17] H. Y. Chen and Y. P. Chu, *Phys. Rev. E* **71**, 010901(R) (2005).
 - [18] F. H. Stillinger and T. A. Weber, *J. Chem. Phys.* **80**, 4434 (1984).
 - [19] D. J. Lacks and M. J. Osborne, *Phys. Rev. Lett.* **93**, 255501 (2004).
 - [20] Z. Y. Guo, D. Thirumalai, and J. D. Honeycutt, *J. Chem. Phys.* **97**, 525 (1992).
 - [21] W. H. Press, S. A. Teukolsky, W. T. Vetterling, and B. P. Flannery, *Numerical Recipes in Fortran*, 2nd ed. (Cambridge University Press, Cambridge, U.K., 1992).
 - [22] P. Hanggi, P. Talkner, and M. Borkovec, *Rev. Mod. Phys.* **62**, 251 (1990).
 - [23] H. Nymeyer, A. Garcia, and J. Onuchic, *Proc. Natl. Acad. Sci. U.S.A.* **95**, 5921 (1998).
 - [24] O. K. Dudko, A. E. Filippov, J. Klafter, and M. Urbakh, *Proc. Natl. Acad. Sci. U.S.A.* **100**, 11378 (2003).
 - [25] Y. J. Sheng, S. Y. Jiang, and H. K. Tsao, *J. Chem. Phys.* **123**, 091102 (2005).
 - [26] C. L. Dias, M. Dube, F. A. Oliveira, and M. Grant, *Phys. Rev. E* **72**, 011918 (2005).
 - [27] W. L. Johnson and K. Samwer, *Phys. Rev. Lett.* **95**, 195501 (2005).
 - [28] G. Hummer and A. Szabo, *Biophys. J.* **85**, 5 (2003).